Title

Maximum Uptake and Hypermetabolic Volume of 18F-FDOPA PET Estimate Molecular Status and Overall Survival in Low-Grade Gliomas: A PET and MRI Study.

Journal

Clinical Nuclear Medicine, 45(12)

ISSN

0363-9762

Authors

Tatekawa, Hiroyuki
Yao, Jingwen
Oughourlian, Talia C
et al.

Publication Date

2020-12-01

DOI

10.1097/rlu.0000000000003318

Peer reviewed

Maximum Uptake and Hypermetabolic Volume of ^{18}F-FDOPA PET Estimate Molecular Status and Overall Survival in Low-Grade Gliomas

A PET and MRI Study

Hiroyuki Tatekawa, MD, PhD,† Jingwen Yao, MS,*†‡ Talia C. Oughourlian, MS,*†§ Akifumi Hagiwara, MD, PhD,*† Chencai Wang, PhD,*† Catalina Raymond, MS,*† Albert Lai, MD, PhD,||¶ Timothy F. Cloughesy, MD,||¶ Phioanh L. Nghiemphu, MD,||¶ Linda M. Liau, MD, PhD, MBA,||** Noriko Salamon, MD, PhD,† and Benjamin M. Ellingson, PhD*†‡§||*

Purpose: We evaluated ^{18}F-FDOPA PET and MRI characteristics in association with the molecular status and overall survival (OS) in a large number of low-grade gliomas (LGGs).

Methods: Eighty-six patients who underwent ^{18}F-FDOPA PET and MRI and were diagnosed with new or recurrent LGGs were retrospectively evaluated with respect to their isocitrate dehydrogenase (IDH) and 1p19q status (10 IDH wild type, 57 mutant, 19 unknown; 1p19q status in IDH mutant: 20 noncodeleted, 37 codeleted). After segmentation of the hyperintense area on fluid-attenuated inversion recovery image ($FLAIR_{ROI}$), the following were calculated: normalized SUVmax (nSUVmax) of ^{18}F-FDOPA relative to the striatum, ^{18}F-FDOPA hypermetabolic volume (tumor-to-striatum ratios >1), $FLAIR_{ROI}$ volume, relative cerebral blood volume, and apparent diffusion coefficient within $FLAIR_{ROI}$. Receiver operating characteristic curve and Cox regression analyses were performed.

Results: PET and MRI metrics combined with age predicted the IDH mutation and 1p19q codeletion statuses with sensitivities of 73% and 76% and specificities of 100% and 94%, respectively. Significant correlations were found between OS and the IDH mutation status (hazard ratio [HR] = 4.939), nSUVmax (HR = 2.827), ^{18}F-FDOPA hypermetabolic volume (HR = 1.048), and $FLAIR_{ROI}$ volume (HR = 1.006). The nSUVmax (HR = 151.6) for newly diagnosed LGGs and the ^{18}F-FDOPA hypermetabolic volume (HR = 1.038) for recurrent LGGs demonstrated significant association with OS.

Conclusions: Combining ^{18}F-FDOPA PET and MRI with age proved useful for predicting the molecular status in patients with LGGs, whereas the nSUVmax and ^{18}F-FDOPA hypermetabolic volume may be useful for prognostication.

Key Words: ^{18}F-FDOPA PET, low-grade glioma, molecular biomarker, overall survival

(*Clin Nucl Med* 2020;00: 00–00)

For clinical evaluation of low-grade gliomas (LGGs), MRI is the primary imaging modality owing to its high spatial resolution, high contrast within soft tissues, and no ionizing radiation. Numerous studies have reported the impact of MRI characteristics on tumor classification and prognosis; however, because of lack of contrast enhancement, LGGs cannot be fully evaluated by MRI alone. Meanwhile, radiolabeled amino acids PET, such as 3,4-dihydroxy-6-[^{18}F]-fluoro-L-phenylalanine (^{18}F-FDOPA), O-(2-[^{18}F] fluoroethyl)-L-tyrosine (^{18}F-FET), and [^{11}C] methyl-L-methionine (^{11}C-MET), is often used in neuro-oncological practice to identify metabolically active tissue.[1] ^{18}F-FDOPA and ^{18}F-FET PET have improved distribution and efficiency owing to the relatively long half-lives of fluorinated tracers compared to carbon tracers.[2] They have been used for the evaluation of LGGs with regard to tumor classification,[3] preoperative biopsy guidance,[4] and prognostication.[5] Because amino acids PET provides metabolic information to complement MRI, a combination of the techniques may yield more accurate observations for differentiating subtypes of LGGs and predicting prognosis than either technique alone.

Villani et al[5] reported that hyper ^{18}F-FDOPA uptake was an independent predictor of progression-free survival; however, they did not evaluate the overall survival (OS). Patel et al[6] demonstrated that the combination of ^{18}F-FDOPA and MRI characteristics is capable of predicting the degree of malignancy and OS among 45 gliomas, including 16 LGGs. The ability of ^{18}F-FDOPA and MRI to predict OS in a large cohort of patients with LGGs has yet to be evaluated. In 2016, the World Health Organization (WHO) glioma classification was modified to include molecular subtypes including isocitrate dehydrogenase (IDH) gene mutations or chromosomal 1p19q codeletion.[7] These molecular biomarkers have become essential for brain tumor classification, treatment decisions, and predicting prognosis for LGGs; however, the features of LGGs with different molecular subtypes are still debated.[3,8] Hence, there is a demand for noninvasive imaging biomarkers that can identify the molecular status and predict OS for LGGs.

Received for publication June 12, 2020; revision accepted August 24, 2020.

From the *UCLA Brain Tumor Imaging Laboratory, Center for Computer Vision and Imaging Biomarkers; †Department of Radiological Science, David Geffen School of Medicine; ‡Department of Bioengineering, Henry Samueli School of Engineering; §Neuroscience Interdepartmental Program; ||UCLA Neuro-Oncology Program; and Departments of ¶Neurology and **Neurosurgery, David Geffen School of Medicine, University of California Los Angeles, Los Angeles, CA.

Conflicts of interest and sources of funding: Funding was received from SNMMI (H.T.), ACS Research Scholar Grant (RSG-15-003-01-CCE: B.M.E.), ABTA Research Collaborators Grant (ARC1700002: B.M.E.), NBTS Research Grant (B.M.E., T.F.C.), NIH/NCI UCLA Brain Tumor SPORE (1P50CA211015-01A1: B.M.E., A.L., T.F.C., P.L.N.), and NIH/NCI (1R21CA223757-01: B.M.E.). B.M.E. is an advisor for Hoffman La-Roche, Siemens, Nativis, Medicenna, MedQIA, Bristol Meyers Squibb, Imaging Endpoints, and Agios Pharmaceuticals. He is a paid consultant for Nativis, MedQIA, Siemens, Hoffman La-Roche, Imaging Endpoints, Medicenna, and Agios. He received grant funding from Siemens, Agios, and Janssen. T.F.C. is on the advisory board for Roche/Genentech, Amgen, Tocagen, NewGen, LPath, Proximagen, Celgene, Vascular Biogenics Ltd, Insys, Agios, Cortice Bioscience, Pfizer, Human Longevity, BMS, Merck, Notable Lab, and MedQIA. None declared for the other authors.

Correspondence to: Benjamin M. Ellingson, PhD, David Geffen School of Medicine, University of California, Los Angeles, 924 Westwood Blvd, Suite 615, Los Angeles, CA 90024. E-mail: bellingson@mednet.ucla.edu.

Supplemental digital content is available for this article. Direct URL citation appears in the printed text and is provided in the HTML and PDF versions of this article on the journal's Web site (www.nuclearmed.com).

ISSN: 0363-9762/20/0000–0000
DOI: 10.1097/RLU.0000000000003318

The purpose of the current study was to evaluate characteristics of LGGs using ^{18}F-FDOPA PET and multiparametric MRI in a large patient cohort and determine associations between imaging metrics and their molecular status or OS.

MATERIALS AND METHODS

Patient Selection

Eighty-six patients with histologically confirmed LGGs with WHO grade II, who underwent ^{18}F-FDOPA PET and MRI scans between 2007 and 2019, were retrospectively included. Selected MRI scans were performed within 2 months of the corresponding PET scans. MR perfusion imaging for 55 subjects and diffusion-weighted imaging for 83 subjects, as well as conventional sequences, were obtained. All patients were diagnosed with new or recurrent LGGs according to the WHO 2007 or 2016 classification. When available, IDH1 mutational status, 1p19q codeletion status, and O_6-methylguanine-DNA methyltransferase (MGMT) promoter methylation status were obtained.[9] For newly diagnosed LGGs, no patients underwent stereotactic biopsy prior to ^{18}F-FDOPA PET or MRI, and the median date between PET scan and surgery/biopsy was 18 days (range, 1–505). Overall survival was measured from the time of the PET scan until death or the censored date (median term, 1272 days). This Health Insurance Portability and Accountability Act–compliant study has been approved by the institutional review board, and all subjects signed an informed consent form. The patient cohort was partly overlapped with a previous study.[10]

^{18}F-FDOPA PET Image Acquisition

A ^{18}F-FDOPA PET scan was performed with a full-ring PET/CT scanner (ECAT-HR; CTI/MIMVista, Siemens, Knoxville, TN) on the subjects, after they fasted for more than 4 hours. Following previously established procedures, ^{18}F-FDOPA was synthesized and injected intravenously.[11] CT images were acquired prior to the PET scan for attenuation correction. Three-dimensional ^{18}F-FDOPA emission data were acquired for a total of 30 minutes and integrated between 10 and 30 minutes following the injection to obtain 20-minute static ^{18}F-FDOPA images. PET images were reconstructed using an ordered-subset expectation maximization iterative reconstruction algorithm, consisting of 6 iterations with 8 subsets.[12] Finally, a Gaussian filter with a full width at half maximum of 4 mm was applied. The resulting voxel size was 1.34 × 1.34 × 3 mm for the ^{18}F-FDOPA PET images. SUV maps of ^{18}F-FDOPA were calculated based on the radioactive activity divided by the decay-corrected injected dose per body mass.[13] The resulting SUV maps were subsequently normalized relative to the median value of the striatum (nSUV).[14]

MRI Acquisition

Anatomical MRI at least consisted of standard T1-weighted precontrast and postcontrast images (2D axial turbo spin echo with 3-mm slice thickness and no interslice gap or 3D inversion prepared gradient echo images with 1- to 1.5-mm isotropic voxel size) and T2-weighted fluid-attenuated inversion recovery (FLAIR) images acquired at 3-mm slice thickness with no interslice gap on a 1.5- or 3-T clinical MRI scanner.

For the dynamic susceptibility contrast perfusion MRI, a total dose of 0.1 mmol/kg of Gd-DTPA or Gd-BTDO3A (Magnevist or Gadavist; Bayer HealthCare Pharmaceuticals, Wayne, NJ) was administered. Relative cerebral blood volume (rCBV) maps were calculated using previously established procedures.[15] Normalized rCBV maps were then computed by dividing the rCBV map by the median rCBV value of regions of interest (ROIs), placed on the contralateral normal-appearing white matter.

Diffusion-weighted imaging was performed by a single-shot echo-planar imaging sequence in the axial plane with $b = 1000$ s/mm^2, slice thickness = 3 mm, and no interslice gap. Apparent diffusion coefficient (ADC) maps were calculated from the acquired images with $b = 1000$ s/mm^2 and $b = 0$ s/mm^2. In the case where diffusion-weighted imaging was not obtained, diffusion tensor imaging was used, acquired from 12 to 64 equidistant diffusion-sensitizing directions with $b = 1000$ s/mm^2 with a single $b = 0$ s/mm^2 image with slice thickness = 2 to 3 mm and no interslice gap. Mean diffusivity maps were used as estimates of the ADC using FSL software (*dtifit*; FMRIB, Oxford, UK; http://www.fmrib.ox.ac.uk/fsl/).

Postprocessing Analysis

All PET and MR images were registered to the corresponding postcontrast T1-weighted images using a 6-degree-of-freedom rigid transformation and a mutual information cost function using FSL (*flirt*). A single ROI as a $FLAIR_{ROI}$ was semiautomatically segmented based on the regions of hyperintensity on the T2-weighted FLAIR images by a board-certificated neuroradiologist (H.T. with 13 years of clinical experience) using Analysis of Functional NeuroImages software (NIMH Scientific and Statistical Computing Core, Bethesda, MD; https://afni.nimh.nih.gov).[16] The nSUVmax was quantified within the $FLAIR_{ROI}$. ^{18}F-FDOPA hypermetabolic volume, including the voxel with nSUV greater than 1 within $FLAIR_{ROI}$, and $FLAIR_{ROI}$ volume were calculated in milliliters. The median rCBV was calculated along with ADC low (ADC_{low}), which is defined as the lower mean of a double Gaussian mixed model fitted to the histogram of ADC values within the $FLAIR_{ROI}$.[17]

Figure 1 illustrates an example of segmentations of $FLAIR_{ROI}$ and the ^{18}F-FDOPA hypermetabolic region in a newly diagnosed 57-year-old male patient with low-grade diffuse glioma.

Statistical Analyses

The Shapiro-Wilk test was used to test for normality of the data. The Student *t* test for normally distributed data and Mann-Whitney *U* test for non–normally distributed data were performed.

Within the $FLAIR_{ROI}$, the evaluation included pairwise Spearman correlation between the nSUVmax, ^{18}F-FDOPA hypermetabolic volume, $FLAIR_{ROI}$ volume, median rCBV, and ADC_{low}, and the comparison of these values with regard to different molecular status (IDH mutation, 1p19q codeletion, and MGMT methylation status) and patient status (newly diagnosed and recurrent). The Kaplan-Meier curves and log-rank test were used to compare OS for different molecular status. A multiple logistic regression model, integrating known clinical information such as age and MR-PET metrics, was used to predict the molecular status. Receiver operating characteristic curves were used to determine whether a combination of clinical and MR-PET imaging information can discriminate between different molecular statuses. Area under the curve (AUC), along with the sensitivity and specificity of differentiation, was evaluated as a measure of model performance. Leave-one-out cross-validation was used to evaluate the accuracy of the multivariate logistic regression model.

Cox univariate regression analyses were conducted to investigate the association between OS and predictor variables including clinical information (sex, age, and molecular status) and imaging metrics (nSUVmax, ^{18}F-FDOPA hypermetabolic volume, $FLAIR_{ROI}$ volume, median rCBV, and ADC_{low}). For the Cox multivariate regression, the hazard of the nSUVmax, ^{18}F-FDOPA hypermetabolic volume, and $FLAIR_{ROI}$ volume controlling for age or molecular status (IDH or 1p19q) were evaluated separately because these three imaging variables were available from all subjects.

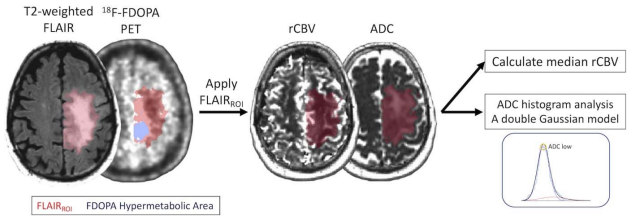

FIGURE 1. Postprocessing and segmentation example. A 57-year-old man with newly diagnosed astrocytic diffuse glioma (WHO grade II, IDH1 mutant, 1p19q noncodeleted, and MGMT methylated status). ROIs of the FLAIR hyperintense region ($FLAIR_{ROI}$, red area) and ^{18}F-FDOPA hypermetabolic area (nSUV >1, blue area) within $FLAIR_{ROI}$ are shown. $nSUV_{max}$ and volumes for each ROI are calculated. $FLAIR_{ROI}$ is copied and pasted on rCBV and ADC maps, and median rCBV and ADC_{low} are calculated.

Additionally, subjects were stratified by molecular status and patient status, and the imaging metrics and their association with OS were evaluated for each subgroup analysis.

Statistical analysis was performed using R software (version 3.5.2; http://www.r-project.org/) and GraphPad Prism (version 8.3; GraphPad Software, La Jolla, Calif). Statistical significance was defined as $P < 0.05$, and no correction for multiple comparisons was performed.

RESULTS

Table 1 summarizes the patient demographics and molecular information, and Supplemental Table 1, http://links.lww.com/CNM/A286 describes this in more detail. The current study included 86 LGG patients (34 females) with a mean age of 43 years. Twenty-nine patients were newly diagnosed, whereas 57 patients had recurrent status. Ten gliomas were IDH wild type (IDH_{wt}), 57 were IDH mutant (IDH_m), and 19 did not have confirmed IDH status. Among the IDH_m gliomas, 20 were 1p19q noncodeleted ($IDH_{m\text{-}noncodel}$), and 37 were 1p19q codeleted ($IDH_{m\text{-}codel}$).

The pairwise Spearman correlation analysis (Fig. 2) between the nSUVmax, ^{18}F-FDOPA hypermetabolic volume, $FLAIR_{ROI}$ volume, median rCBV, and ADC_{low} demonstrated a strong correlation between the nSUVmax and ^{18}F-FDOPA hypermetabolic volume ($r_s = 0.90$), whereas the other pairs had weak or no correlations ($-0.24 < r_s < 0.37$).

In the evaluation of patients stratified by the molecular status (Fig. 3), the Kaplan-Meier curves and log-rank tests showed significant differences in the OS ($P = 0.01$). The $IDH_{m\text{-}codel}$ subtype had the longest OS, followed by the $IDH_{m\text{-}noncodel}$ subtype, and the IDH_{wt} subtype had the worst OS. When comparing the imaging metrics, the nSUVmax ($P = 0.033$) and ^{18}F-FDOPA hypermetabolic volume ($P = 0.043$) were significantly higher in $IDH_{m\text{-}codel}$ than $IDH_{m\text{-}noncodel}$. Other analyses did not yield any significant differences between the different molecular subtypes (all $P > 0.06$). The evaluation between MGMT unmethylated and methylated subtypes is shown in Supplemental Figure 1, http://links.lww.com/CNM/A286.

Subsequently, we tested whether the combination of the MR and PET imaging metrics and patient age can be used to predict the molecular status. We created a new metric from a combination of the imaging factors and patient age by incorporating a multiple logistic regression model as follows:

$$\ln\left[\frac{P(\text{wt})}{P(\text{m})}\right] = 0.295 \times (\text{Age}) - 0.820 \times (\text{nSUV}_{\text{max}}) - 0.241 \times (\text{FDOPA hypermetabolic volume [mL]}) + 1.026 \times 10^{-2} \times (\text{FLAIR}_{\text{ROI}}\text{volume [mL]}) + 0.966 \times (\text{rCBV}) + 1.783 \times 10^{-2}\,(\text{ADC}_{\text{low}}[\times 10^{-6}]) - \underbrace{34.90}_{\text{Intercept}}$$

This metric enabled to differentiate the IDH mutation status (AUC, 0.93; sensitivity, 73%; specificity, 100%), with only patient age as a significant factor (odds ratio = 1.34, $P = 0.04$). Leave-one-out classification accuracy to differentiate IDH mutation was 86% (sensitivity, 97%; specificity, 71%). Similarly, for prediction of the 1p19q codeletion status, a multiple logistic regression analysis was performed as follows:

$$\ln\left[\frac{P(\text{codel})}{P(\text{noncodel})}\right] = 0.237 \times (\text{Age}) + 1.360 \times (\text{nSUV}_{\text{max}}) + 0.148 \times (\text{FDOPA hypermetabolic volume [mL]}) - 0.760 \times (\text{FLAIR}_{\text{ROI}}\text{ volume [mL]}) - 0.721 \times (\text{rCBV}) - 1.102 \times 10^{-3} \times (\text{ADC}_{\text{low}}[\times 10^{-6}]) - \underbrace{7.111}_{\text{Intercept}}$$

This metric enabled to differentiate the 1p19q codeletion status (AUC, 0.91; sensitivity, 76%; specificity, 94%), with patient age

TABLE 1. Patient Demographics and Molecular Information

No. patients		86
Female		34 (39.5%)
Age ± SD, y		43.8 ± 12.6
IDH mutation and 1p19q codeletion status	IDH wild type	10 (11.6%)
	IDH mutant 1p19q noncodeleted	20 (23.2%)
	IDH mutant 1p19q codeleted	37 (43.0%)
	Unknown	19 (22.1%)
MGMT promoter methylation status	Unmethylated	17 (19.8%)
	Methylated	25 (29.1%)
	Unknown	44 (51.2%)
Patient status	Newly diagnosed	29 (33.7%)
	Recurrent	57 (66.3%)

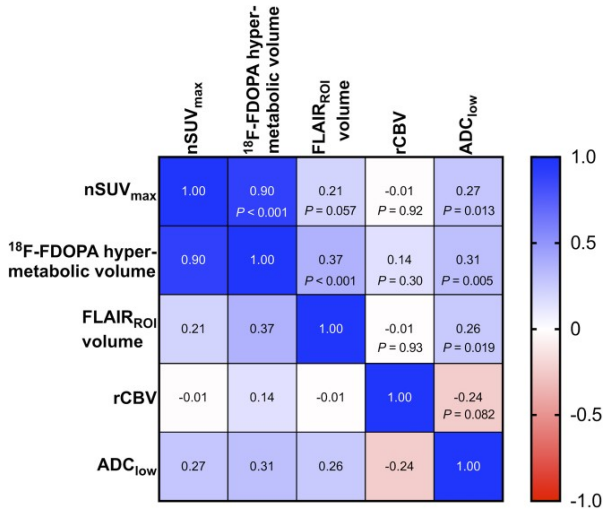

FIGURE 2. Pairwise Spearman correlation matrix between nSUVmax, ^{18}F-FDOPA hypermetabolic volume, $FLAIR_{ROI}$ volume, median rCBV, and ADC_{low}.

(odds ratio = 1.27, P = 0.011) and $FLAIR_{ROI}$ volume (odds ratio = 0.93, P = 0.019) being significant factors. Leave-one-out classification accuracy to differentiate 1p19q codeletion was 65% (sensitivity, 63%; specificity, 67%). Receiver operating characteristic curves to predict IDH or 1p19q status were also evaluated using only the patient age, only PET metrics (ie, nSUVmax and ^{18}F-FDOPA hypermetabolic volume), only MRI metrics (ie, $FLAIR_{ROI}$ volume, median rCBV, and ADC_{low}), or combined PET and MRI metrics. The AUC of IDH or 1p19q status was higher using both PET and MRI parameters than when using either of the parameters individually; however, the AUC incorporating patient age and MR-PET parameters yielded the highest value.

When stratifying the patients into newly diagnosed and recurrent LGGs (Fig. 4), the nSUVmax, ^{18}F-FDOPA hypermetabolic volume, and ADC_{low} were significantly higher in the recurrent LGGs than newly diagnosed LGGs (P < 0.001, <0.001, and 0.016, respectively). Further subgroup analyses, stratified by molecular status (IDH_{wt}, $IDH_{m\text{-}noncodel}$, and $IDH_{m\text{-}codel}$) and patient status (newly diagnosed and recurrent), are shown in Supplemental Figure 2, http://links.lww.com/CNM/A288 and exhibited similar trends with higher nSUVmax and ^{18}F-FDOPA hypermetabolic volume in $IDH_{m\text{-}codel}$ than $IDH_{m\text{-}noncodel}$ in both newly diagnosed and recurrent groups, although they were not significant.

The Cox univariate analysis (Table 2) showed a significant increase in hazard associated with the IDH status (hazard ratio [HR] = 4.939, 95% confidence interval [CI] = 1.203–20.28, P = 0.026), nSUVmax (HR = 2.827, CI = 1.202–6.649, P = 0.017), ^{18}F-FDOPA hypermetabolic volume (HR = 1.048, CI = 1.019–1.078, P = 0.001), and $FLAIR_{ROI}$ volume (HR = 1.006, CI = 1.000–1.013, P = 0.046). The Cox multivariate regression analysis controlling for age showed a significant increase in the hazard associated with the nSUVmax (HR = 3.208, CI = 1.272–8.090, P = 0.013) and ^{18}F-FDOPA hypermetabolic volume (HR = 1.045, CI = 1.017–1.073, P = 0.001), but not with FLAIR volume (HR = 1.006, CI = 0.999–1.013, P = 0.08). When controlling for IDH status or 1p19q status (for IDH_m LGGs), the Cox multivariate regression analysis showed a significant increase in the hazard of OS associated with the nSUVmax (controlling for IDH status: HR = 4.101, CI = 1.244–13.53, P = 0.020; controlling for 1p19q status: HR = 6.169, CI = 1.537–24.76, P = 0.010) and ^{18}F-FDOPA hypermetabolic volume (controlling for IDH status: HR = 1.063, CI = 1.005–1.125, P = 0.032; controlling for 1p19q status: HR = 1.097, CI = 1.021–1.180, P = 0.011), but not with FLAIR volume (controlling for IDH status: HR = 1.002, CI = 0.981–1.024, P = 0.83; controlling for 1p19q: HR = 1.003, CI = 0.981–1.025, P = 0.80). Subgroup analysis stratified by different molecular status or patient status demonstrated that the nSUVmax represented an independent predictor of OS for $IDH_{m\text{-}noncodel}$ (HR = 6.100, CI = 1.155–32.22, P = 0.033) and newly diagnosed LGGs (HR = 151.6, CI = 1.289–17,830, P = 0.038), whereas the increases in the ^{18}F-FDOPA hypermetabolic volumes (HR = 1.038, CI = 1.009–1.067, P = 0.009) and $FLAIR_{ROI}$ volumes (HR = 1.006, CI = 1.000–1.013, P = 0.049) were independent predictors for recurrent LGGs (Supplemental Table 2, http://links.lww.com/CNM/A289).

DISCUSSION

In the current study, ^{18}F-FDOPA PET and MRI characteristics were evaluated with regard to their association with molecular status and OS in LGG patients. Our investigation revealed that combining PET and MRI information with patient age could predict IDH and 1p19q status more accurately than using PET or MRI information alone. We also confirmed that nSUVmax and ^{18}F-FDOPA hypermetabolic volume were higher in $IDH_{m\text{-}codel}$ than $IDH_{m\text{-}noncodel}$ LGGs. The Cox regression analysis revealed significant associations of OS with the IDH status, nSUVmax, ^{18}F-FDOPA hypermetabolic volume, and $FLAIR_{ROI}$ volume. Because not all recurrent glioma patients in all institutions have a known molecular status at the time point of the previous surgery or biopsy, the results of predicting

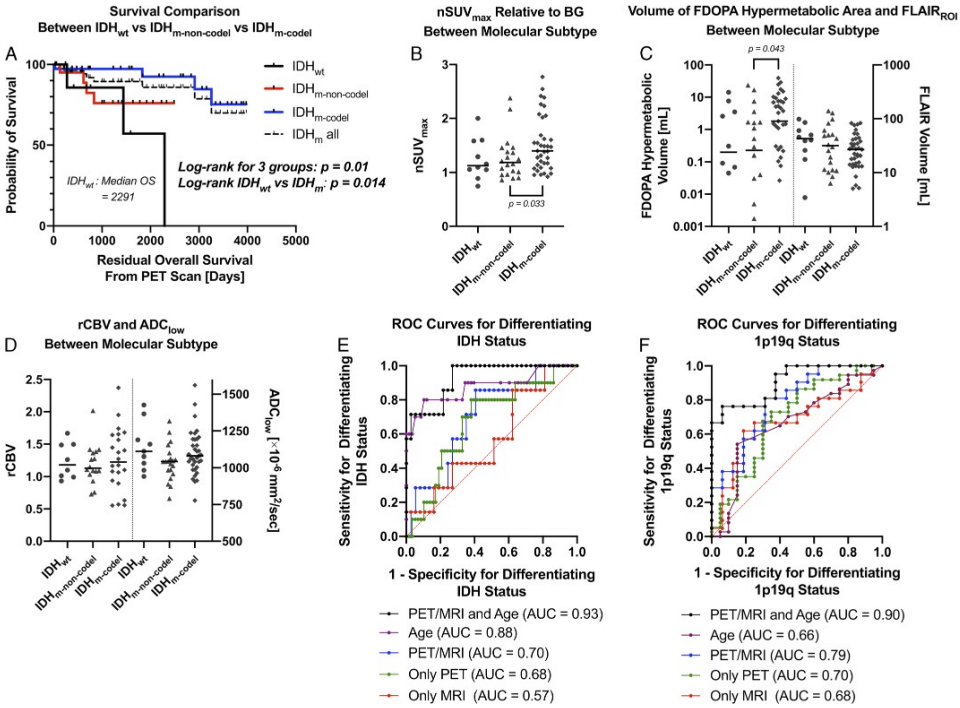

FIGURE 3. **A**, Kaplan-Meier plots showing significant differences in OS between IDH_{wt}, $IDH_{m\text{-}noncodel}$, and $IDH_{m\text{-}codel}$ gliomas, or between IDH_{wt} and IDH_m. **B**, The nSUVmax and (**C**) volume of ^{18}F-FDOPA hypermetabolic area and $FLAIR_{ROI}$ and (**D**) median rCBV and ADC_{low} between different molecular statuses. The nSUVmax and ^{18}F-FDOPA hypermetabolic volume are significantly higher in $IDH_{m\text{-}codel}$ than $IDH_{m\text{-}noncodel}$. When comparing between IDH_{wt} and IDH_m (including $IDH_{m\text{-}noncodel}$ and $IDH_{m\text{-}codel}$), no imaging metrics show significant differences. Receiver operating characteristic curves for differentiating (**E**) IDH mutation or (**F**) 1p19q codeletion status using patient age and imaging information, only age, both PET and MRI, only PET, or only MRI.

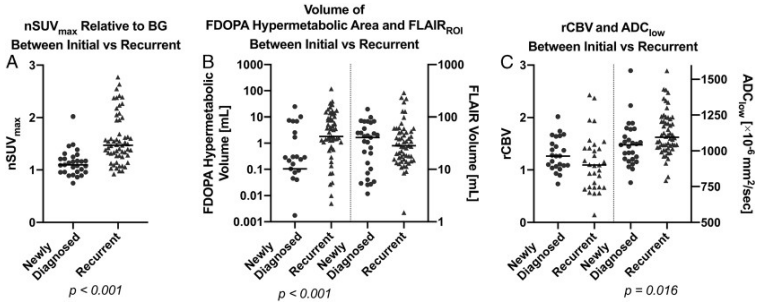

FIGURE 4. **A**, The nSUVmax, (**B**) volume of ^{18}F-FDOPA hypermetabolic area or $FLAIR_{ROI}$, and (**C**) median rCBV and ADC_{low} between newly diagnosed and recurrent LGGs.

TABLE 2. Cox Univariate Regression

	Cox Univariate Regression		
	HR	95% CI	*P*
Sex	1.579	0.551–4.517	0.39
Age (y)	1.03	0.996–1.064	0.083
IDH status (wild type vs mutant)	4.939	1.203–20.28	0.026*
1p19q status for IDH mutant (noncodel vs codel)	0.234	0.042–1.301	0.097
MGMT status (unmethylated vs methylated)	0.56	0.078–4.001	0.56
Patient status (newly diagnosed vs recurrent)	2.231	0.640–7.766	0.2
nSUVmax	2.827	1.202–6.649	0.017*
FDOPA hypermetabolic volume (mL)	1.048	1.019–1.078	0.001*
$FLAIR_{ROI}$ volume (mL)	1.006	1.000–1.013	0.046*
rCBV	1.05	0.214–5.151	0.95
ADC_{low} ($\times 10^{-6}$ mm^2/s)	1.002	0.999–1.005	0.17

*Statistically significant.

molecular status and prognosis are useful not only for newly diagnosed LGGs, but also for recurrent LGGs.

The molecular status of LGGs is crucial for patient diagnosis and predicting prognosis. As shown previously and in this study, the IDH mutation status was significantly associated with OS with shorter survival for IDH_{wt} LGGs due to the biological similarities to glioblastomas.[8,18] In the evaluation of imaging metrics of LGGs, although some studies have evaluated the association of amino acid tracer uptake and molecular status, the imaging features in different molecular status were not confirmed. One study stratified gliomas into IDH_{wt} and IDH_m groups, which included 1p19q noncodeleted and codeleted gliomas and showed higher tracer uptake in IDH_m than IDH_{wt}.[3] Other studies stratified gliomas into 1p19q codeleted and noncodeleted groups, which included both $IDH_{m\text{-}noncodel}$ and IDH_{wt} gliomas, and showed no significant differences between 1p19q codeleted and noncodeleted gliomas.[19,20] The diverse patient cohort in each study may confuse the issue and mask the associations of the amino acid tracer uptake with molecular status. In contrast, the current study stratified gliomas into three groups (IDH_{wt}, $IDH_{m\text{-}noncodel}$, and $IDH_{m\text{-}codel}$) and confirmed the features of amino acid tracer uptake, including higher nSUVmax and ^{18}F-FDOPA hypermetabolic volume in $IDH_{m\text{-}codel}$ than $IDH_{m\text{-}noncodel}$ LGGs. This was consistent with previous literature indicating a higher tracer uptake in oligodendrogliomas compared with astrocytomas, reflecting higher cell density, endothelial hyperplasia, microvascular proliferation, and higher vascular bed in oligodendroglial compared with astrocytic components.[8,10,21,22] When comparing between IDH_{wt} and IDH_m, the ratio of $IDH_{m\text{-}codel}$ LGGs in the IDH_m group may affect the differences of ^{18}F-FDOPA uptake because the current study revealed $IDH_{m\text{-}codel}$ LGGs to show high tracer uptake.

In the current study, the combination of PET and MRI information with patient age successfully differentiated the IDH mutation and 1p19q codeletion status with AUCs higher than 0.90, although the performance, particularly for the IDH mutation status, was largely dependent on the patient age. A previous study revealed that the $IDH_{m\text{-}noncodel}$ group tended to be found in the youngest patients, followed by $IDH_{m\text{-}codel}$ and IDH_{wt}[23]; hence, the combination of PET and MRI, along with patient age, may be helpful for predicting the molecular status.

High ^{18}F-FDOPA uptakes are known to reflect high metabolic activity and predict worse survival outcomes in both newly diagnosed and recurrent gliomas.[6,24] For glioblastomas, hypermetabolic volume was an important factor.[25] For newly diagnosed LGGs, the uptake of amino acid tracers was reported to be associated with progression-free survival[5,8] and predicted disease progression after 1-year follow-up.[26] No studies have revealed the association of ^{18}F-FDOPA uptake and OS in grade II gliomas alone, partly due to a small cohort population. The current large cohort study revealed that increased nSUVmax of ^{18}F-FDOPA was associated with a worse prognosis in grade II gliomas; furthermore, the ^{18}F-FDOPA hypermetabolic volume was also associated with a worse prognosis. These results were consistent with the strong correlation between the nSUVmax and ^{18}F-FDOPA hypermetabolic volume, detected in this study. Previous studies have indicated that the volume of the contrast-enhancing regions was predictive of the OS[27]; however, because of the lack of contrast enhancement, such regions cannot be evaluated in most grade II gliomas. Meanwhile, because hypermetabolic volume can be calculated regardless of contrast enhancement, it could be a useful biomarker for gliomas, especially for non–contrast-enhancing LGGs.

When comparing the newly diagnosed and recurrent LGGs, both nSUVmax and ^{18}F-FDOPA hypermetabolic volume were significantly higher in recurrent LGGs. The treatment-related changes may have affected amino acid tracer uptake, because ^{18}F-FDOPA uptake in normal-appearing brain structures might be altered by temozolomide treatment.[28] The blood-brain barrier breakdown, due to cancer progression, may contribute to the extent of amino acid transport in recurrent gliomas, suggesting that the SUV may not directly reflect recurrent tumor activity.[29] Malignant transformation at recurrence may also induce an increase in the SUV in some LGGs.[24] Unfortunately, the histopathology of recurrent tumors was not available for all patients, and thus it was not analyzed in this study. Several studies evaluated the longitudinal change of amino acids tracer uptake, reporting that a higher rate of temporal change in the ^{18}F-FDOPA uptake was associated with a higher risk of malignant transformation and poor survival in patients with LGGs.[9] A study reported that 65% of primary gliomas with a negative ^{18}F-FET uptake, which could not be delineated from the background brain tissue, turned PET-positive during follow-up scans, indicating that gliomas can change their ^{18}F-FET uptake behavior throughout the course of the disease.[30] Although ^{18}F-FET PET–negative gliomas in general have a better prognosis than ^{18}F-FET positive gliomas, ^{18}F-FET PET–negative gliomas with photopenic defects were reported to have a higher risk of harboring a higher-grade glioma and an unfavorable outcome than gliomas with indifferent ^{18}F-FET uptake to the background.[31,32] Meanwhile, this study exhibited a better prognosis in patients with lower ^{18}F-FDOPA uptake, and no studies have reported such unfavorable outcomes for ^{18}F-FDOPA hypouptake gliomas. The different disease courses may be caused by different amino acid tracers, in particular different metabolic processes of ^{18}F-FDOPA and ^{18}F-FET. Hence, comparison of the glioma pathology and amino acid uptakes with different tracers is desirable, in a longitudinal manner.

The retrospective nature of this study presents one of its limitations; specifically, the clinical information (Karnofsky Performance Status), molecular status, and rCBV/ADC maps were not obtained for all subjects, and the imaging protocols were not exactly matched. Although examination and treatment planning were discussed in weekly tumor boards at our institution, the patient cohort was potentially influenced by selection bias because FDOPA PET examination may have been performed more often for glioma patients who were suspected to have primary or recurrent gliomas but were difficult to be diagnosed based on conventional MRI alone. For three patients with newly diagnosed LGGs, the interval between PET and surgery/biopsy was longer than half a year; however, they did not receive additional treatments between the interval, and the WHO grades remained at grade II when the pathology was confirmed after surgery. Nonetheless, the possibility of temporal change in

molecular status during the interval cannot be excluded. Including patients with various previous treatment statuses may have influenced the MRI and/or PET imaging features. As we could not obtain pathologies of all recurrent gliomas after the PET examination, the WHO grade may have been underestimated. Although this study used leave-one-out cross-validation for evaluating the predictive performance of molecular status, another independent cohort is required to generalize our classification performance.

CONCLUSIONS

This was the largest population study to date evaluating LGGs using both ^{18}F-FDOPA PET and MRI. A combination of PET, MRI, and patient age may be helpful for predicting the molecular status in patients with LGGs, and ^{18}F-FDOPA PET metrics proved useful for estimating the OS.

REFERENCES

1. Galldiks N, Lohmann P, Cicone F, et al. FET and FDOPA PET imaging in glioma. In: Pope W, ed. *Glioma Imaging*. 1st ed. Cham, Switzerland: Springer Nature Switzerland AG; 2019:211–222.
2. Huang C, McConathy J. Radiolabeled amino acids for oncologic imaging. *J Nucl Med*. 2013;54:1007–1010.
3. Verger A, Metellus P, Sala Q, et al. IDH mutation is paradoxically associated with higher ^{18} F-FDOPA PET uptake in diffuse grade II and grade III gliomas. *Eur J Nucl Med Mol Imaging*. 2017;44:1306–1311.
4. Kunz M, Thon N, Eigenbrod S, et al. Hot spots in dynamic (18)FET-PET delineate malignant tumor parts within suspected WHO grade II gliomas. *Neuro Oncol*. 2011;13:307–316.
5. Villani V, Carapella CM, Chiaravalloti A, et al. The role of PET [^{18}F]FDOPA in evaluating low-grade glioma. *Anticancer Res*. 2015;35:5117–5122.
6. Patel CB, Fazzari E, Chakhoyan A, et al. ^{18}F-FDOPA PET and MRI characteristics correlate with degree of malignancy and predict survival in treatment-naive gliomas: a cross-sectional study. *J Neurooncol*. 2018;139:399–409.
7. Louis DN, Perry A, Reifenberger G, et al. The 2016 World Health Organization classification of tumors of the central nervous system: a summary. *Acta Neuropathol*. 2016;131:803–820.
8. Kertels O, Kessler AF, Mihovilovic MI, et al. Prognostic value of O-(2-[^{18} F] fluoroethyl)-L-tyrosine PET/CT in newly diagnosed WHO 2016 grade II and III glioma. *Mol Imaging Biol*. 2019;21:1174–1181.
9. Oughourlian TC, Yao J, Schlossman J, et al. Rate of change in maximum ^{18} F-FDOPA PET uptake and non-enhancing tumor volume predict malignant transformation and overall survival in low-grade gliomas. *J Neurooncol*. 2020;147:135–145.
10. Tatekawa H, Hagiwara A, Yao J, et al. Voxel-wise and patient-wise correlation of ^{18}F-FDOPA PET, rCBV, and ADC in treatment-naïve diffuse gliomas with different molecular subtypes [published online July 9, 2020]. *J Nucl Med*. 2020.
11. Bishop A, Satyamurthy N, Bida G, et al. Proton irradiation of [^{18}O]O_2: production of [^{18}F]F_2 and [^{18}F]F_2 + [^{18}F] OF_2. *Nucl Med Biol*. 1996;23:189–199.
12. Nuyts J, Michel C, Dupont P. Maximum-likelihood expectation-maximization reconstruction of sinograms with arbitrary noise distribution using NEC-transformations. *IEEE Trans Med Imaging*. 2001;20:365–375.
13. Thie JA. Understanding the standardized uptake value, its methods, and implications for usage. *J Nucl Med*. 2004;45:1431–1434.
14. Chen W, Silverman DH, Delaloye S, et al. ^{18}F-FDOPA PET imaging of brain tumors: comparison study with ^{18}F-FDG PET and evaluation of diagnostic accuracy. *J Nucl Med*. 2006;47:904–911.
15. Leu K, Boxerman JL, Lai A, et al. Bidirectional contrast agent leakage correction of dynamic susceptibility contrast (DSC)–MRI improves cerebral blood volume estimation and survival prediction in recurrent glioblastoma treated with bevacizumab. *J Magn Reson Imaging*. 2016;44:1229–1237.
16. Ellingson BM, Kim HJ, Woodworth DC, et al. Recurrent glioblastoma treated with bevacizumab: contrast-enhanced T1-weighted subtraction maps improve tumor delineation and aid prediction of survival in a multicenter clinical trial. *Radiology*. 2014;271:200–210.
17. Pope WB, Kim HJ, Huo J, et al. Recurrent glioblastoma multiforme: ADC histogram analysis predicts response to bevacizumab treatment. *Radiology*. 2009;252:182–189.
18. Olar A, Wani KM, Alfaro-Munoz KD, et al. IDH mutation status and role of WHO grade and mitotic index in overall survival in grade II–III diffuse gliomas. *Acta Neuropathol*. 2015;129:585–596.
19. Cicone F, Carideo L, Scaringi C, et al. ^{18}F-DOPA uptake does not correlate with IDH mutation status and 1p/19q co-deletion in glioma. *Ann Nucl Med*. 2019;33:295–302.
20. Yao J, Hagiwara A, Raymond C, et al. Human IDH mutant 1p/19q co-deleted gliomas have low tumor acidity as evidenced by molecular MRI and PET: a retrospective study. *Sci Rep*. 2020;10:11922.
21. Kobayashi K, Hirata K, Yamaguchi S, et al. Prognostic value of volume-based measurements on (11)C-methionine PET in glioma patients. *Eur J Nucl Med Mol Imaging*. 2015;42:1071–1080.
22. Naslund O, Smits A, Forander P, et al. Amino acid tracers in PET imaging of diffuse low-grade gliomas: a systematic review of preoperative applications. *Acta Neurochir*. 2018;160:1451–1460.
23. Eckel-Passow JE, Lachance DH, Molinaro AM, et al. Glioma groups based on 1p/19q, IDH, and TERT promoter mutations in tumors. *N Engl J Med*. 2015;372:2499–2508.
24. Karunanithi S, Sharma P, Kumar A, et al. Can (18)F-FDOPA PET/CT predict survival in patients with suspected recurrent glioma? A prospective study. *Eur J Radiol*. 2014;83:219–225.
25. Suchorska B, Jansen NL, Linn J, et al. Biological tumor volume in ^{18}FET-PET before radiochemotherapy correlates with survival in GBM. *Neurology*. 2015;84:710–719.
26. Rossi Espagnet MC, Romano A, Mancuso V, et al. Multiparametric evaluation of low grade gliomas at follow-up: comparison between diffusion and perfusion MR with (18)F-FDOPA PET. *Br J Radiol*. 2016;89:20160476.
27. Ellingson BM, Wen PY, Cloughesy TF. Evidence and context of use for contrast enhancement as a surrogate of disease burden and treatment response in malignant glioma. *Neuro Oncol*. 2018;20:457–471.
28. Carideo L, Minniti G, Mamede M, et al. ^{18}F-DOPA uptake parameters in glioma: effects of patients' characteristics and prior treatment history. *Br J Radiol*. 2018;91:20170847.
29. Fueger BJ, Czernin J, Cloughesy T, et al. Correlation of 6-^{18}F-fluoro-L-dopa PET uptake with proliferation and tumor grade in newly diagnosed and recurrent gliomas. *J Nucl Med*. 2010;51:1532–1538.
30. Unterrainer M, Schweisthal F, Suchorska B, et al. Serial ^{18}F-FET PET imaging of primarily ^{18}F-FET–negative glioma: does it make sense? *J Nucl Med*. 2016;57:1177–1182.
31. Galldiks N, Unterrainer M, Judov N, et al. Photopenic defects on O-(2-[^{18}F]-fluoroethyl)-L-tyrosine PET: clinical relevance in glioma patients. *Neuro Oncol*. 2019;21:1331–1338.
32. Jansen NL, Suchorska B, Wenter V, et al. Dynamic ^{18}F-FET PET in newly diagnosed astrocytic low-grade glioma identifies high-risk patients. *J Nucl Med*. 2014;55:198–203.